

Homogenisation procedure to evaluate the effectiveness of masonry strengthening by CFRP repointing technique

A. CECCHI, A. BARBIERI

Dipartimento di Costruzione dell'Architettura

Università IUAV di Venezia

Dorsoduro, 2206 - Venezia

ITALIA

cecchi@iuav.it; barbieri@iuav.it; <http://www.iuav.it>

Abstract: - In this work masonry walls, made of clay bricks and mortar joints, have been investigated and in particular the effectiveness of CFRP repointing technique is analysed by homogenisation procedure. Masonry walls - typical of historical buildings and churches - are subject to in plane or/and out of plane loading and, due to the low tensile strength of mortar joint (assumed zero in terms of safety), need strengthening procedure to bearing seismic loads or new service loads related to restoration design. The homogenisation procedure has been carried out taking into account several geometrical and mechanical parameters of masonry and CFRP strengthening. The difficulty in modelling masonry lies in its heterogeneous character, since it is composed by blocks between which mortar joints are laid. Here a linear elastic analysis is performed that is significant under service loads, and may be a starting point for non linear and collapse analysis.

The masonry has been identified with a standard elastic continuum by means of homogenisation method. Two homogenisation approaches are proposed: an analytical approach and a numerical approach. Both of them allow to determine values of homogenised in plane moduli, for running bond texture, strengthened by CFRP, taking into account the effective micro-structure of masonry and FRP

An extensive numerical analysis has been carried out to investigate the reliability of homogenisation methods to take into account the geometrical and mechanical parameters in the analysis of masonry walls considering different FRP Young moduli. The sensitivity of strain field to strengthening material is investigated on a meaningful case such as a masonry wall loaded by horizontal and vertical displacement respectively along horizontal joints or vertical ones. This case is of practical interest for the partition masonry walls: *infill walls*.

Key-Words: - Masonry, CFRP repointing, Homogenisation, in plane moduli.

1 Introduction

The conservation of historical heritage is an important topic in Italy, due to relevant amount of historical and monumental buildings in the country and seismic events occurred in the centuries. Hence, a branch of scientific research concerns the evaluation of suitable strengthening techniques able to preserve these structures for the future generations. In the last two decades new materials and techniques have been developed in the building market to strength existing structures and reinforce the new ones, e.g. FRP materials (Fiber Reinforced Polimers).

Some load conditions request tensile strength in masonry elements. FRP materials represent a possible solution because of their negligible weight compared with high tensile strength, if loaded along the fibre direction. Moreover, the FRP application is not invasive because it could be removed by mechanical and thermal action (temperature increment). The use of composite materials is an

effective technique able to preserve historical buildings without modifying their structural behaviour under service conditions. Hence FRP technology is interesting from structural and economical points of view because it offers a wide range of mechanical characteristics and a ratio strength/weight very high respect to other traditional materials (reinforced concrete and steel).

In the present research, running bond texture is assumed as reference, because it often characterises historical masonries. CFRP (Carbon Fiber Reinforced Polimers) strip is assumed as strengthening material of bed mortar joints and the CFRP repointing technique is considered. It consists of embedding continuous FRP strip in the horizontal joint of a wall by suitable paste; the horizontal joint is previously grooved, hence the masonry texture has to present continuous horizontal joints, as in the running bond courses. In this research, the case of CFRP strip inserted along the whole masonry thickness is studied. Few studies has been carried out on this technique [1, 2, 3, 4]. In masonry

structures, this technique is proposed to control the cracking phenomena in historical masonry structure. Generally these cracks appear on the point of the failure. Some study cases are in progress on bell towers and masonry columns of some historical monuments in Italy [5, 6].

A previous research of the authors, to apply homogenisation procedure, was carried out to analyse bearing masonry columns and to evaluate their axial and flexural homogenised moduli [7]. The masonry columns are not strengthened but sensitivity to different textures, at a macroscopic structural level was investigated.

Several studies have been carried out to develop a model for masonries in plane loaded, reinforced with CFRP sheets [8, 9]. In these studies the strengthening material is bonded to lateral surfaces of masonry; the strengthened masonry may be considered as a multilayer material (CFRP sheet - masonry- CFRP sheet). Here, for CFRP repointing technique, an analogous model is proposed following the same methodology. In this case the mechanical properties of strengthened masonry are still obtained by homogenisation procedure but the multilayer approach, obviously, may not be applied. In fact, the strengthening material is part of the bed joint along the masonry thickness. The homogenisation approach links the masonry behaviour on the micro-level to the macro-level, to take into account global and local phenomena in terms of stress and/or strain distribution [10, 11], as CFRP strengthening [9]. The homogenisation approach starts considering mechanical and geometrical properties of single masonry constituents (blocks and mortar joints) as of CFRP strengthening material and identifies an elementary cell, which regular repetition describes the body as a whole. In this way the field problem is led to the unit cell, reducing the computation effort and carrying out average values of mechanical properties.

The mechanical and geometrical characteristics of masonry should be different and this aspect is influent on mechanical parameters. The analytical model proposed in [12] is meaningful because it provides explicit equations for elastic in plane moduli. Moreover in the present research the model in [12] is implemented. In fact the effective joint thickness is taken into account; while in the previous paper of Cecchi and Sab [12] the case of zero thickness joint was investigated. Hence, a comparison between the in plane moduli obtained with zero joint thickness and finite joint thickness is carried out. Furthermore, 2D homogenised F.E. model is performed in which mortar joint un-

strengthened and strengthened is modelled as a standard continuous and not as in the analytical model as an interface.

To evaluate the reliability of the 2D homogenised models, a 2D heterogeneous F.E. model has been performed. A numerical analysis has been carried out by comparing the strain field at specific cross sections of an in plane loaded masonry wall, which bed joints are strengthened by CFRP strip repointing technique. The carried out analysis is relative to the case of not bearing walls with running bond texture. Two boundary and loading conditions are considered: 1) masonry panel fixed at the base and loaded by an horizontal unit displacement at the top - bed joint direction; 2) masonry panel fixed at the left side and loaded by an horizontal unit displacement at the right side - head joint direction.

2 The FRP repointing technique

Generally partition masonry walls (infill walls) are considered as non-structural elements and they are not taken into account in the restoration or building design. Nevertheless, these structures may contribute to the structural response as a whole, in particular under seismic events. This aspect is evinced in the Eurocode 8 [13]. The necessity to reduce the vulnerability of infill masonry walls is evident and different techniques are available today; one of these is the repointing technique. This technique is recently re-proposed by the researchers substituting the traditional steel bars with truss type steel reinforcement [14] or CFRP strips. This technique is used to strength masonry wall in plane and out of plane loaded. The first application is to resist shear cracking as shown in figure 1.



Figure 1. Crack pattern of masonry wall subjected to seismic event.

The CFRP repointing may be used to connect adjacent bearing walls and increase the

collaboration between them for in plane and out of plane loading. A typical example is the failure mechanism of bell towers due to horizontal force. Generally two opposite wall are loaded in plane (shear loading) whereas the other two are loaded out of plane (bending loading). A good connection between walls may increase the structural capacity of the structure as a whole. The failure mechanism is generally that shown in figure 2.



Figure 2. Crack pattern of masonry bell tower subjected to seismic event.

CFRP repointing technique brings to both structural and practical advantages as:

- 1) strengthening material can be easily inserted in the horizontal joint;
- 2) strengthening material is protected against corrosion;
- 3) technique may be applied as reinforcement in new construction and as strengthening in retrofitting historical ones;
- 4) strengthening material is effective in cracking control;
- 5) same technique can increase the in plane and out of plane capacity.

In the present research the in plane capacity is analysed.

3 Field problem in homogenisation procedure

Heterogeneous materials may be modelled using homogenisation techniques. This permits the definition of an homogeneous body, equivalent to the heterogeneous one in its geometry and in the properties of its constituent materials. The application of these techniques is tied to the assumption of body "periodic" structure; then the body is obtained by regular repetition of non-homogeneous REV (Representative Elementary

Volume), whose dimensions are small relative to the overall size of the body itself.

Several studies exist on the homogenisation of un-reinforced masonry and reinforced masonry with FRP sheets (e.g. [8], [9], [10]); here the research is focused to masonry strengthened by CFRP repointing technique.

Only the horizontal joints are strengthened by insertion of CFRP strip along their cross section; while the vertical joints are still homogeneous and isotropic.

The horizontal joints are non homogeneous - CFRP material embedded in mortar joint-, and their constitutive function becomes orthotropic due to the CFRP fibre direction. The research focuses on masonry walls with running bond texture, loaded only in plane and strengthened along the whole cross section of bed joint. The analytical and numerical analyses are carried on considering plane stress and plane strain hypotheses. The homogenisation procedure is based on the solution of the following auxiliary problem on the elementary cell:

$$\begin{cases} \operatorname{div} \boldsymbol{\sigma} = 0 \\ \boldsymbol{\sigma} = \mathbf{a}(y) \boldsymbol{\varepsilon} \\ \boldsymbol{\varepsilon} = \mathbf{E} + \operatorname{sym}(\operatorname{grad} \mathbf{u}^{per}) \\ \boldsymbol{\sigma} \mathbf{e}_\alpha \text{ anti-periodic on } \partial Y \\ \mathbf{u}^{per} \text{ periodic on } \partial Y \end{cases} \quad (1)$$

where ∂Y is the boundary of the Y -REV, as in the next sections will be defined; $\boldsymbol{\sigma}$ is the Cauchy stress tensor; $\boldsymbol{\varepsilon}$ is the microscopic in plane strain tensor; \mathbf{E} is the macroscopic in plane strain tensor and \mathbf{u}^{per} is a periodic displacement field on ∂Y ; \mathbf{a} is the constitutive function defined as: \mathbf{a}^B for $y \in \text{block}$ and \mathbf{a}^J for $y \in \text{joint}$, with \mathbf{a}^B and \mathbf{a}^J are respectively the block and the joint constitutive law.

Considering in plane loading, the solution of the field problem (1) permits to evaluate the homogenised constitutive law of the panel - macroscopic homogenised functions -. In the general case the average operation provides the following macroscopic constitutive relation:

$$\mathbf{N} = \langle \boldsymbol{\sigma} \rangle = \mathbf{A}^H \mathbf{E} + \mathbf{B}^H \boldsymbol{\chi} \quad (2)$$

where \mathbf{N} is the in plane force tensor, \mathbf{A}^H and \mathbf{B}^H are the constitutive homogenised moduli, $\boldsymbol{\chi}$ is the curvature tensor and $\langle \cdot \rangle$ is the average operator defined as:

$$\langle f \rangle = \frac{1}{t_i} \int_{t_i} f(y_1, y_2) dy_1 dy_2 \quad (3)$$

where t_i is the dimension of Y -REV.

Due to the symmetry of the problem, the homogenised constitutive law (2) should be simplified, because $\mathbf{B}^H = 0$, hence:

$$\mathbf{N} = \langle \boldsymbol{\sigma} \rangle = \mathbf{A}^H \mathbf{E} \quad (4)$$

or in terms of the components:

$$\mathbf{N}_{\alpha\beta} = \langle \boldsymbol{\sigma}_{\alpha\beta} \rangle = \mathbf{A}_{\alpha\beta\gamma\delta}^H \mathbf{E}_{\gamma\delta} \quad (5)$$

where Greek index $\alpha, \beta = 1, 2$. At this stage the macroscopic field problem at the structural level may be built.

In that follows, this 2D problem is carried out in term of plane stress or plane strain hypothesis, defining the lower and upper bound of the 3D solution. This one will be enclosed between the lower bound and upper bound curves.

4 Analytical homogenisation procedure

An analytical simplified model has been proposed by Cecchi and Rizzi [15] and implemented by Cecchi and Sab [12, 16] considering three perturbative parameters:

- $\varepsilon = l/L$ ratio between the l size of the cell and the L dimension of the overall panel ;
- $\beta = e/l$ ratio between the e joint thickness and the l size of the cell.
- $\xi = E^m/E^b$, ratio between the E^m mortar Young modulus and the E^b block Young modulus;

The aim of analytical models are to obtain in a symbolic form the expressions of $\mathbf{A}_{\alpha\beta\gamma\delta}^H$ homogenised moduli.

In the present research, only the first two parameters are considered. In [12, 15] the mortar joint is considered as an interface with zero thickness and with a constitutive function that is directly obtained as a linear function of the displacement jump across the joint. Here the finite joint thickness is considered, whereas the constitutive function is still defined as in [12]. Hence the strain measure, in the joints, is still the $[\mathbf{u}]$ jump of displacement across the joint itself. In the un-strengthened case the constitutive function of joints is:

$$\mathbf{K} = \frac{1}{e} (\mu^M \mathbf{I} + (\mu^M + \lambda^M) (\mathbf{n} \otimes \mathbf{n})) \quad (6)$$

where e is the joint thickness and in particular e_v is the vertical joint thickness, e_h is the horizontal joint thickness, \mathbf{n} is the normal to the interface, μ^M and λ^M are the Lamé constants of mortar. The index h and v may be also referred to the linear constitutive function \mathbf{K} . It must be noted the diagonal form of the \mathbf{K} tensor. Hence, due to small size of e if

compared with other dimensions of the joint, the transversal contraction is negligible and may not be taken in account, while in the standard continuous, as well known, is not negligible.

The aim is to implement the model proposed by Cecchi and Sab [12] considering the finite joint thickness.

Let be (\mathbf{x}) a reference system for the global description of the masonry wall, called \mathfrak{S} in the macroscopic scale and let be (\mathbf{y}) a reference system for the elementary module Y -REV. The Y module, as shown in figure 3 may be defined as:

$$Y = \left] -\frac{t_1}{2}, \frac{t_1}{2} \right[\times \left] -\frac{t_2}{2}, \frac{t_2}{2} \right[= \omega \quad (7)$$

where t_i are the 2 dimensions of Y , according to 2 axes directions; ω is the middle plane of masonry panel.

The field problem (1) becomes:

$$\left\{ \begin{array}{l} \text{div} \boldsymbol{\sigma} = 0 \\ \boldsymbol{\sigma} = \mathbf{a}^B \boldsymbol{\varepsilon} \\ \boldsymbol{\varepsilon} = \mathbf{E} + \text{sym}(\text{grad} \mathbf{u}^{per}) \\ \boldsymbol{\sigma} \mathbf{e}_\alpha \text{ anti-periodic on } \partial Y \\ \mathbf{u}^{per} \text{ periodic on } \partial Y \\ [\mathbf{u}] \neq 0 \text{ discontinuous for } y \in \Sigma \\ [\boldsymbol{\sigma} \mathbf{n}] = 0 \text{ continuous for } y \in \Sigma \\ \boldsymbol{\sigma} \mathbf{n} = \mathbf{K}[\mathbf{u}] \text{ interface constitutive function} \\ \text{for } y \in \Sigma \end{array} \right. \quad (8)$$

where ∂Y is the boundary of the Y -REV, \mathbf{a}^B is the constitutive function for $y \in \text{block}$, $[\mathbf{u}]$ is the jump of displacement at the finite thickness interface and Σ is the interface; \mathbf{K} is the constitutive function of the finite thickness joint, according to (6).

Comparing the procedure proposed by Cecchi and Sab [12] -zero joint thickness- and the procedure here proposed -finite joint thickness-, the homogenised moduli for elastic blocks and joints are obtained in Y -REV and not in Y_b -REV - where Y_b is the area of the REV referred to the only blocks -.

In figure 4 the mesh used for the symbolic solution of field problem (8) is shown.

In order to solve the field problem on the characteristic elementary pattern, it has been meshed into just 10 finite elements to obtain an estimate in symbolic form of the homogenised elastic moduli, taking the identification between the nodes owing to the assumption of the above-mentioned periodicity conditions. The elements chosen are triangular with three nodes and the mesh used, in order to take the discontinuities of the

displacement field across the finite joint, entails the presence of two nodes at the points A, A*, B, B*, C and D, in fact the discontinuity are AB, A*B* and CD. Besides the periodicity conditions on the displacement field entail an identification between the points A-A* and B-B*.

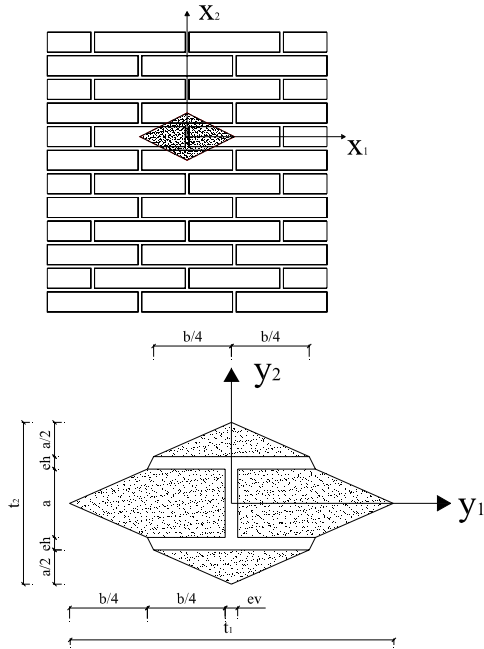


Figure 3 The *Y-REV* for the analytical homogenisation model: *Y-REV*, in the masonry panel, and detail of *Y-REV*.

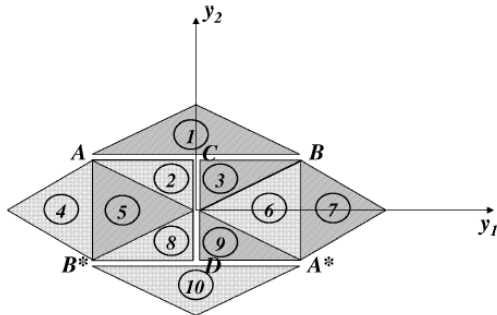


Figure 4 Mesh of *Y-REV* for the estimation of in plane moduli by analytical model.

Respect to the Cecchi and Sab paper A-A* and B-B* are not coincident i.e. two point are considered and the distance is respectively e_h or e_v . The problem formulated below has been handled in symbolic form, using a mathematical software.

4.1 Influence of joint thickness

In the following paragraph the results carried out by the analytical model formulated by Cecchi and Sab [12] are compared with those carried out by the here

proposed finite joint thickness model for the un-strengthened masonry.

The homogenised moduli for elastic brick and joint are obtained in *Y-REV* following the procedure of Cecchi and Sab [12] but the model is implemented for finite joint dimensions e_h and e_v , respectively bed and head joints. Hence it is:

$$\begin{aligned}
 A_{1111}^H &= \frac{a}{a+e_h} \left(A_{1111}^B K' + \mathbf{B} \frac{e_h}{a} \right) \left(4K' \frac{e_h}{a+e_h} + \frac{b+e_v}{a+e_h} K'' \frac{e_v}{a+e_h} \right) \\
 &\quad \frac{4 \frac{e_h^2}{(a+e_h)^2} \frac{e_v}{b+e_v} \mathbf{B} + A_{1111}^B \frac{e_h}{a+e_h} \mathbf{C} + K' \mathbf{D}}{A_{2222}^B K' + \mathbf{B} \frac{e_h}{b+e_v}} \\
 A_{2222}^H &= K' \frac{A_{2222}^B K' + \mathbf{B} \frac{e_h}{b+e_v}}{\frac{e_h}{a+e_h} \frac{e_v}{b+e_v} \mathbf{B} + A_{2222}^B \left(\frac{e_h}{a+e_h} + \frac{e_v}{b+e_v} \right) K' + K'^2} \\
 A_{1122}^H &= \frac{A_{1122}^B K' \frac{a}{a+e_h} \left(4K' \frac{e_h}{a+e_h} + \frac{b+e_v}{a+e_h} K'' \frac{e_v}{a+e_h} \right)}{4 \frac{e_h^2}{(a+e_h)^2} \frac{e_v}{b+e_v} \mathbf{B} + A_{1111}^B \frac{e_h}{a+e_h} \mathbf{C} + K' \mathbf{D}} \\
 A_{1212}^H &= \frac{A_{1212}^B K'' \left(K' \frac{e_v}{b+e_v} + 4 \frac{a+e_h}{b+e_v} K'' \frac{e_h}{b+e_v} \right)}{A_{1212}^B \frac{e_h}{a+e_h} \mathbf{F} + 2K'' \mathbf{G}}
 \end{aligned} \tag{9}$$

where

$$\begin{aligned}
 \mathbf{B} &= (A_{1111}^B)^2 - (A_{1122}^B)^2 \\
 \mathbf{C} &= 4K' \frac{e_h}{a+e_h} + \frac{b+e_v}{a+e_h} K'' \frac{e_v}{a+e_h} + 4K' \frac{a}{a+e_h} \frac{e_v}{b+e_v} \\
 \mathbf{D} &= \frac{a}{a+e_h} \left(4K' \frac{e_h}{a+e_h} + \frac{b+e_v}{a+e_h} K'' \frac{e_v}{a+e_h} \right) \\
 \mathbf{F} &= K' \frac{e_v}{a+e_h} + 4 \frac{a+e_h}{b+e_v} K'' \frac{e_h}{b+e_v} + 4 \frac{(a+e_h)^2}{(b+e_v)^2} K'' \frac{e_v}{b+e_v} \\
 \mathbf{G} &= K' \frac{e_v}{b+e_v} + 4 \frac{a+e_h}{b+e_v} K'' \frac{e_h}{b+e_v}
 \end{aligned}$$

$K' = 2\mu^M + \lambda^M$, $K'' = \mu^M$ and μ^M , λ^M are the mortar Lamè constants under in plane strain hypothesis.

The obtained homogenised constitutive functions, if compared with those of [12], show exactly the same structure, the differences lie in the ratios e_v/b and e_h/a which are substituted respectively by $e_v/(b+e_v)$ and $e_h/(a+e_h)$.

The diagrams for each $A_{\alpha\beta\gamma\delta}^H$ in plane modulus are plotted in figures 5, 6, 7 and 8, under plane strain (PE) and plane stress (PS) hypotheses, comparing the results carried out applying the model with zero joint thickness and that with finite joint thickness. In ordinate the homogenised modulus, both with zero thickness joint ($A_{\alpha\beta\gamma\delta}^H$) and finite thickness joint ($A_{\alpha\beta\gamma\delta}^G$) normalised versus the $A_{\alpha\beta\gamma\delta}^b$ in plane modulus of homogeneous masonry made of block ($E^b=90$ GPa), is reported. In abscissa the ξ^{-1} ($=E^b/E^m$) ratio between the E^b brick Young modulus and the E^m mortar Young modulus is reported.

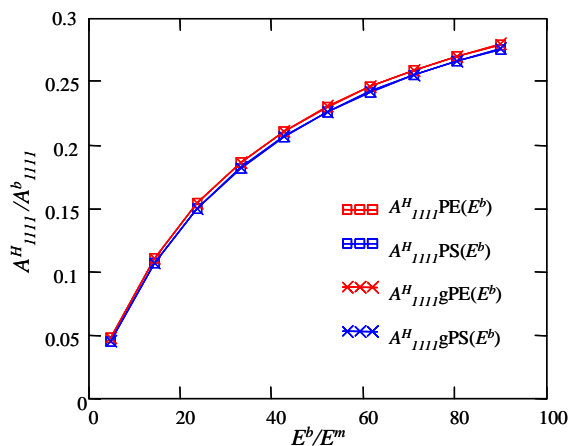


Figure 5 Ratio between A^H_{1111} and A^b_{1111} versus ξ^{-1} .

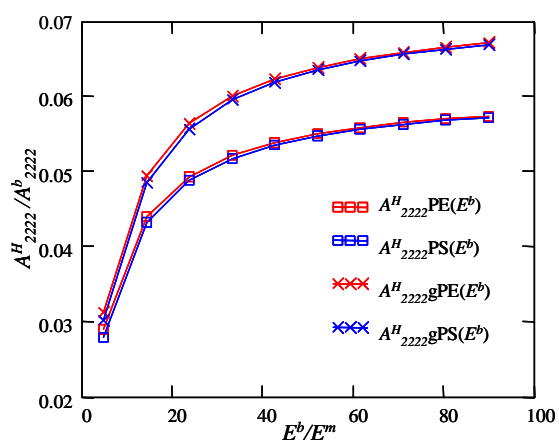


Figure 6 Ratio between A^H_{2222} and A^b_{2222} versus ξ^{-1} .

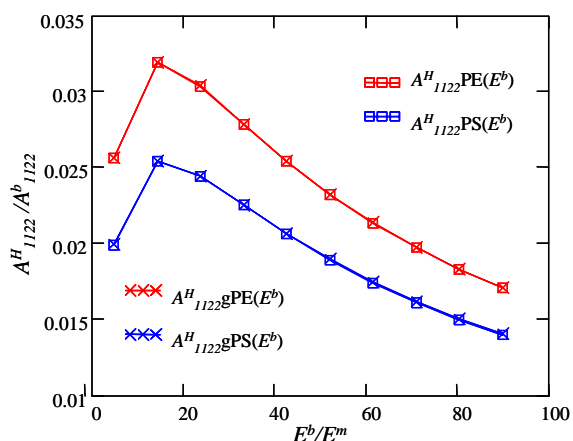


Figure 7 Ratio between A^H_{1122} and A^b_{1122} versus ξ^{-1} .

The investigation evinced that the A^H_{1111} modulus is not influenced by the thickness of joint because the vertical joint is one time present along y_1 axis direction, as shown in the Y -REV of figure 3. Analogous considerations should be done for in plane A^H_{1122} modulus. The joint thickness has different effect on A^H_{2222} and A^H_{1212} moduli. The homogenised elastic constants are bigger than those obtained applying expressions reported in [12]. The

relevant effect of joint thickness is due to that the horizontal joint is present two times along y_2 axis direction (figure 3).

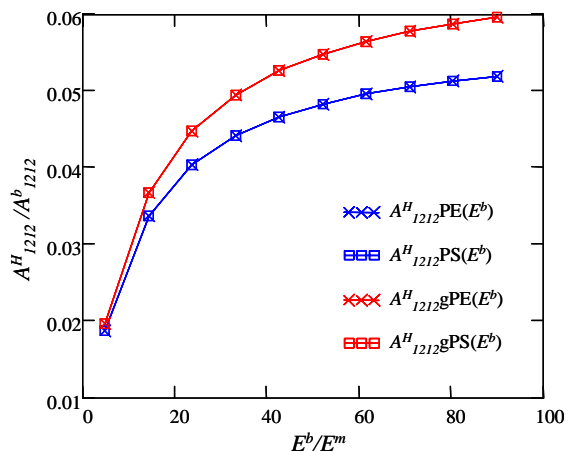


Figure 8 Ratio between A^H_{1212} and A^b_{1212} versus ξ^{-1} .

The error done, considering a zero or finite joint thickness may be evaluated by:

$$err = \frac{A^H_{\alpha\beta\gamma\delta} g - A^H_{\alpha\beta\gamma\delta}}{A^H_{\alpha\beta\gamma\delta} g} \cdot 100 \quad (10)$$

where $A^H_{\alpha\beta\gamma\delta} g$ is the in plane modulus evaluated considering finite joint thickness and $A^H_{\alpha\beta\gamma\delta}$ is the in plane modulus evaluated considering zero joint thickness.

This error, in the evaluation of A^H_{1111} and A^H_{1122} , varies from 0.03% -for $\xi^{-1}=5$ - to 0.19% -for $\xi^{-1}=90$ -; the error obtained in the evaluation of A^H_{2222} varies from 7% -for $\xi^{-1}=5$ - to 14% -for $\xi^{-1}=90$ -, whereas for A^H_{1212} varies from 5% -for $\xi^{-1}=5$ - to 13% - for $\xi^{-1}=90$ -.

The estimation of error allows to observe that the proposed model fits well the results carried out considering model with zero joint thickness for low value of ξ^{-1} : the error estimation is lower than 10%. The ratio between the Young modulus of masonry constituents is relevant in the application of one model or the other. In fact the A^H_{2222} and A^H_{1212} in plane moduli carried out by the proposed model are generally higher than that of [12]. The finite joint thickness in the proposed model increases the stiffness of masonry when the ξ^{-1} ratio increases.

5 F.E. Homogenisation procedure

A numerical method was applied to evaluate the homogenised in plane moduli $A^H_{\alpha\beta\gamma\delta}$ of masonry wall un-strengthened and strengthened by CFRP repointing technique. The numerical analysis is carried out considering a 2D F.E. model for the Y -

REV both under in plane strain hypothesis (upper bound) and under in plane stress hypothesis (lower bound).

The elementary cell chosen here for the numerical model is different respect to the one chosen for the analytical model. The auxiliary field problem on the elementary cell, plotted by dashed line - due to the symmetry - may be reported to the only *Y/4-REV* (Fig. 9).

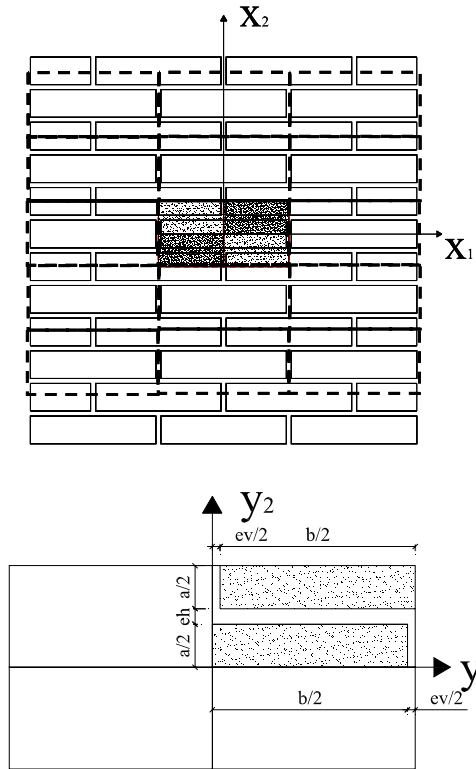


Figure 9 *Y-REV* for the numerical homogenisation procedure: *Y-REV* in the masonry panel, and the detail of *Y-REV*.

The 2D field problem that must be solved is (1) with the following periodic boundary conditions:

$$\mathbf{u} = \begin{pmatrix} E_{11}y_1 + E_{12}y_2 \\ E_{21}y_1 + E_{22}y_2 \end{pmatrix} + \mathbf{u}^{per}(\mathbf{y}) \quad (11)$$

with $E_{12}=E_{21}$.

Hence, the condition $E_{11} \neq 0, E_{22}=E_{12}=0$ provides:

- axial elongation along y_1 axis:

$$u_1 = E_{11}y_1 + u_1^{per}(\mathbf{y}) \quad (12)$$

the condition $E_{22} \neq 0, E_{11}=E_{12}=0$ provides:

- axial elongation along y_2 axis:

$$u_2 = E_{22}y_2 + u_2^{per}(\mathbf{y}) \quad (13)$$

and the condition $E_{12} \neq 0, E_{22}=E_{11}=0$ provides:

- shear deformation along y_1 axis and y_2 axis:

$$u_1 = E_{12}y_2 + u_1^{per}(\mathbf{y}) \quad (14)$$

$$u_2 = E_{21}y_1 + u_2^{per}(\mathbf{y})$$

The boundary conditions that must be imposed in the F.E. model to evaluate the in plane moduli $A_{1111}^H, A_{2222}^H, A_{1122}^H$ and A_{1212}^H are reported in table 1 according to eq. (12)-(13)-(14).

	$y_1 = 0$	$y_1 = t_2/2$	$y_2 = 0$	$y_2 = t_2/2$
A_{1111}^H	$u_1 = 0$	$u_1 = E_{11} \cdot t_1/2$	$u_2 = 0$	-----
A_{2222}^H	$u_1 = 0$	-----	$u_2 = 0$	$u_2 = E_{22} \cdot t_2/2$
A_{1122}^H	$u_1 = 0$	$u_1 = E_{11} \cdot t_1/2$	$u_2 = 0$	-----
A_{2211}^H	$u_1 = 0$	-----	$u_2 = 0$	$u_2 = E_{22} \cdot t_2/2$
A_{1212}^H	$u_2 = 0$	$u_2 = E_{12} \cdot t_1/2$	$u_1 = 0$	$u_1 = E_{12} \cdot t_2/2$

Table 1: Applied boundary conditions at F.E. model.

The imposed suitable boundary conditions for \mathbf{u}^{per} periodic on ∂Y are plotted in figure 10.

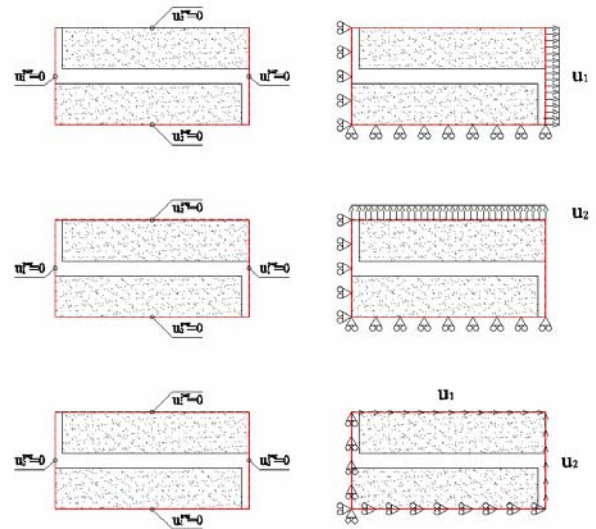


Figure 10 boundary displacement conditions on 2D *Y/4-REV*.

The *Y/4-REV* is defined as follows:

$$Y/4 = \left] 0, \frac{t_1}{2} \right[\times \left] 0, \frac{t_2}{2} \right[\quad (15)$$

The homogenised in plane moduli are evaluated by numerical model on the *Y/4-REV* solving field problem (1). Hence according to equations (3)-(4)-(5) the homogenised constitutive function may be obtained:

$$A_{\alpha\beta\gamma\delta}^H = \frac{1}{\omega} \int \sigma_{\alpha\beta} dA \quad (16)$$

where ω is the middle plane of elementary cell.

The finite element model has been built both for un-strengthened masonry and strengthened masonry, meshing the *Y/4-REV*. Three elements are used in the discretisation of the mortar joint across its thickness: element mortar (4.4 mm), element CFRP (1.2 mm) and element mortar (4.4 mm).

Mortar, block and CFRP are modelled by 4 nodes 2D plane elements. The constitutive laws for mortar, brick and CFRP are linear elastic and isotropic.

6 Masonry property

The analysed masonry is made of UNI clay bricks (250x120x55 mm³), whereas the mortar joint thickness is $e_v=10$ mm for head joint and $e_h=10$ mm for bed joint in the case of un-strengthened masonry. When the strengthened masonry is considered, the horizontal joint thickness is composed of two mortar layer 4.4 mm thick and one central layer of CFRP material 1.2 mm thick. In fact the CFRP repointing technique reduces the mortar bed joint thickness in the measure of the CFRP thickness. The whole thickness of bed joint is still 10 mm.

The mechanical properties of materials in F.E. model are reported in table 2.

Young modulus [MPa]	Poisson ratio
$E^b = 5000 \div 90000$	$\nu^b = 0.2$
$E^m = 1000$	$\nu^m = 0.2$
$E^{FRP} = 145 \cdot 10^3; 210 \cdot 10^3; 300 \cdot 10^3$	$\nu^{FRP} = 0.4$

Table 2: Mechanical properties of materials (b =block; m =mortar; FRP = Fiber Reinforced Polymers).

7 Numerical experimentations

The analytical results carried out considering finite joint thickness, have been compared with the numerical ones. The comparison has been carried on for the un-strengthened case.

Finally, the numerical analysis has been performed for strengthened masonry. The in plane moduli of un-strengthened and strengthened masonry have been evaluated to show the sensitivity of masonry macroscopic behaviour to CFRP repointing technique. The analysis has been carried out for FRP with different longitudinal elastic modulus, as reported in table 2. The aim is to evaluate the increment in terms of in plane stiffness due to CFRP repointing technique and the influence of different FRP axial stiffness respect to the homogenised moduli of strengthened masonry.

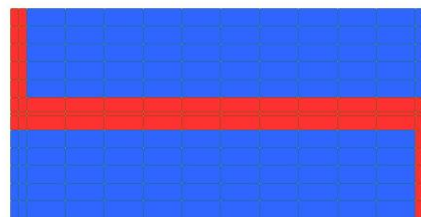


Figure 11 F.E. 2D heterogeneous model: *Y/4-REV* mesh for un-strengthened masonry.

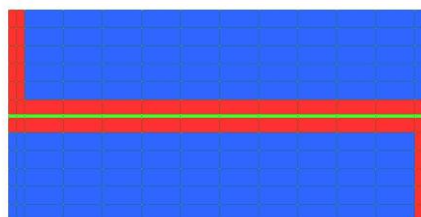


Figure 12 F.E. 2D heterogeneous model: *Y/4-REV* mesh for strengthened masonry by CFRP repointing technique.

The elementary cell - *Y/4-REV* - is meshed by 182 2D plane elements:

- 1- un-strengthened masonry *Y/4-REV*: 120 F.E. elements for modelling brick and 62 F.E. elements for modelling mortar joint;
- 2- strengthened masonry *Y/4-REV*; 120 F.E. elements for modelling brick, 48 F.E. elements for modelling mortar joint and 14 F.E. elements for modelling CFRP.

In figures 11 and 12, the mesh of *Y/4*, respectively for un-strengthened and strengthened masonry, is reported. The mesh of un-strengthened and strengthened cell is the same; the difference is in the mechanical properties of the second layer of horizontal joint elements. In the case of un-strengthened masonry, the mechanical properties are those of mortar and, in the case of strengthened one, the mechanical properties are those of FRP strip.

7.1 Comparison between analytical and numerical results.

The analytical and numerical models have been compared considering the finite joint thickness model.

The diagrams for each $A_{\alpha\beta\gamma\delta}^H$ in plane modulus are plotted in figures 13, 14, 15 and 16, under plane strain (PE) and plane stress (PS) hypotheses. In abscissa the ξ^{-1} ($=E^b/E^m$) ratio between the E^b brick Young modulus and the E^m mortar Young modulus is reported, in ordinate both the ratio between the $A_{\alpha\beta\gamma\delta}^H_{NUM}$ homogenised numerical modulus and the $A_{\alpha\beta\gamma\delta}^b$ in plane modulus of homogeneous masonry made of block ($E^b=90$ GPa) and the ratio

between the $A_{\alpha\beta\gamma\delta}^H$ _AN homogenised analytical modulus and the $A_{\alpha\beta\gamma\delta}^b$ in plane modulus of homogeneous masonry made of block ($E^b=90$ GPa) is reported.

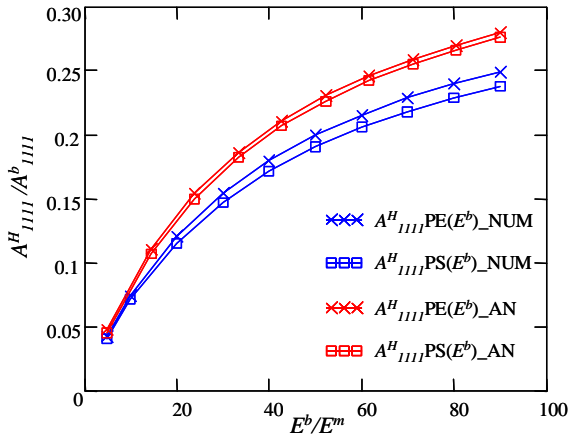


Figure 13 Ratio between A^H_{1111} and A^b_{1111} versus ξ^{-1} for the numerical and analytical models.

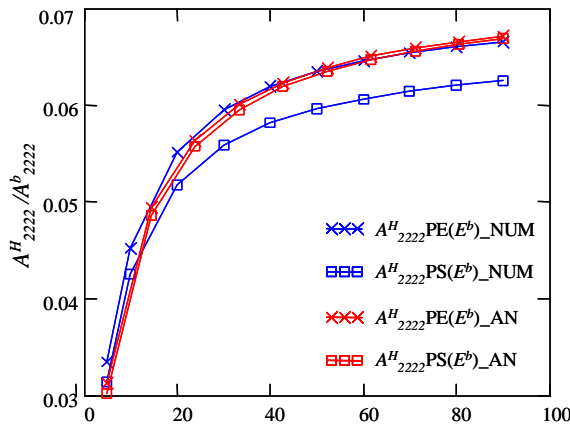


Figure 14 Ratio between A^H_{2222} and A^b_{2222} versus ξ^{-1} for the numerical and analytical models.

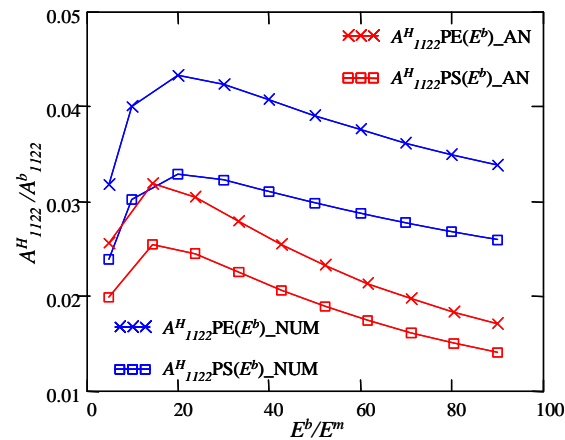


Figure 15 Ratio between A^H_{1122} and A^b_{1122} versus ξ^{-1} for the numerical and analytical models.

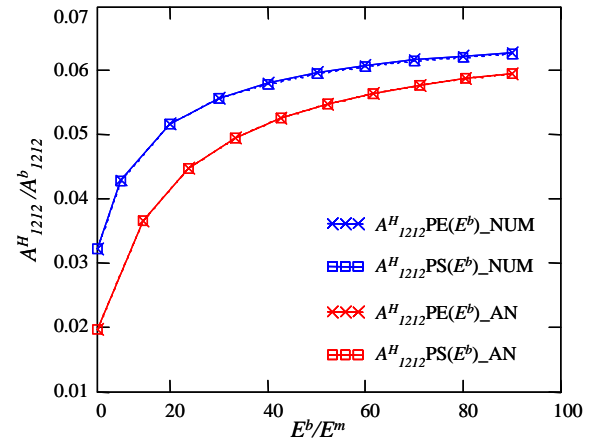


Figure 16 Ratio between A^H_{1212} and A^b_{1212} versus ξ^{-1} for the numerical and analytical models.

The following remarks may be pointed out:

- A^H_{1111} in plane modulus evaluated analytically (AN) is bigger than the one evaluated numerically (NUM) and the difference increases when ξ^{-1} increases.
- A^H_{2222} in plane modulus evaluated analytically is included between the ones evaluated numerically, under in plane strain and in plane stress hypothesis. The values are close to numerical diagram obtained under plane strain hypothesis.
- A^H_{1122} in plane modulus evaluated numerically is bigger than the one evaluated analytically. The variability range between plane strain and plane stress hypothesis is more evident in the numerical model.
- A^H_{1212} in plane modulus evaluated under in plane strain and in plane stress hypothesis does not differ both in the analytical and numerical models. Also in this case the numerical model evaluates a value bigger than the analytical one, but the difference decreases when ξ^{-1} increases.

Generally, the differences between the in plane moduli evaluated under in plane strain and in plane stress hypotheses are bigger in numerical model than in analytical one. These differences are more evident in A^H_{2222} and A^H_{1122} moduli, whereas there is no difference between the two hypotheses in the evaluation of A^H_{1212} , both for analytical and numerical model. This is due to the constitutive function used for modelling the joint in the analytical model: the joint constitutive functions are always evaluated under in plane strain hypothesis while the block constitutive functions changes: in plane strain and in plane stress hypothesis. On the contrary in the numerical model the constitutive function is under in plane stress or under in plane strain hypothesis both for block and for joint.

7.2 Sensitivity to CFRP repointing technique

In this paragraph the sensitivity to CFRP repointing technique is analysed. The numerical analysis has been carried out comparing the un-strengthened masonry with the strengthened one. FRP materials which differ for longitudinal Young modulus: S ($E_{FRP}=145$ GPa); M ($E_{FRP}=210$ GPa); H ($E_{FRP}=300$ GPa) have been assumed.

The efficiency of CFRP repointing technique is shown in the following diagrams (Fig. 17, 18, 19, 20).

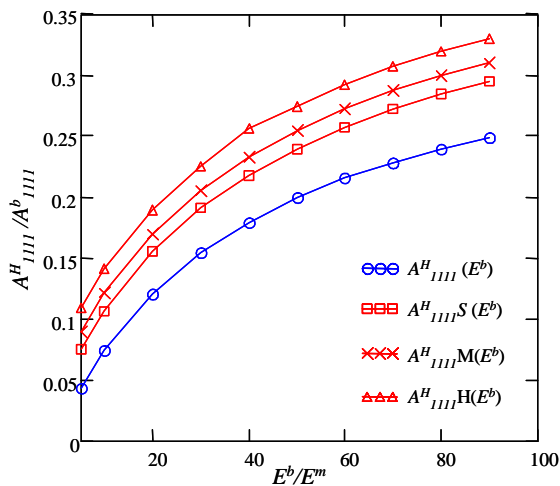


Figure 17 Ratio between A^H_{1111} and A^b_{1111} versus ξ^{-1} comparing un-strengthened and strengthened masonry.

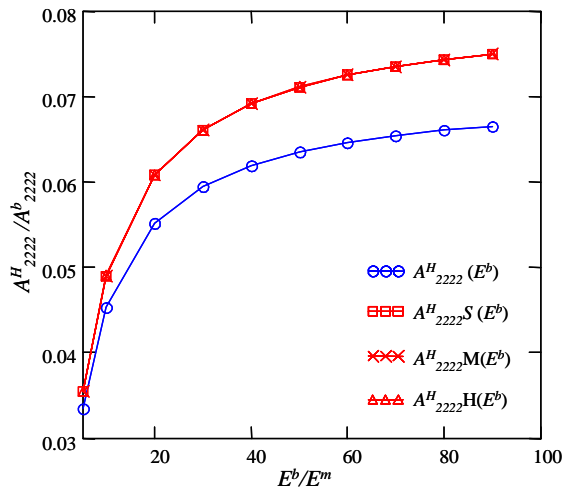


Figure 18 Ratio between A^H_{2222} and A^b_{2222} versus ξ^{-1} comparing un-strengthened and strengthened masonry.

The increment of in plane stiffness in masonry panel is more evident along y_1 axis direction. The A^H_{1111} in plane modulus increases when the E_{FRP} - FRP longitudinal stiffness - increases (Fig. 17),

whereas FRP stiffness is not relevant on the others in plane moduli (Fig. 18, 19, 20). The increment of in plane stiffness is function of the ratio between block modulus and mortar modulus. In fact increasing the value of ξ^{-1} the difference between the un-strengthened value and the strengthened one increases too. The increment is more evident in the A^H_{2222} , A^H_{1122} , and A^H_{1212} in plane moduli. The evaluation of this aspect will be analysed in the following.

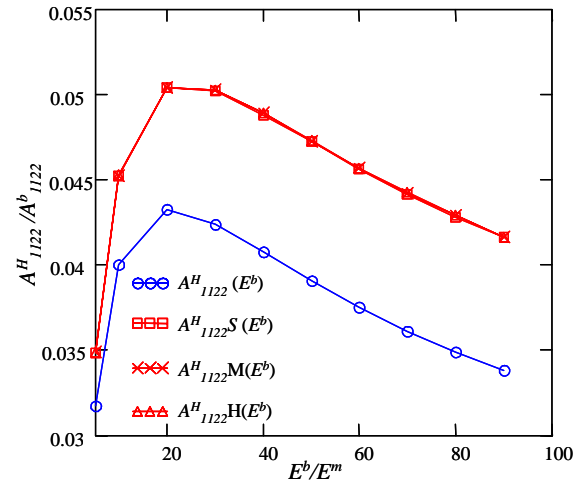


Figure 19 Ratio between A^H_{1122} and A^b_{1122} versus ξ^{-1} comparing un-strengthened and strengthened masonry.

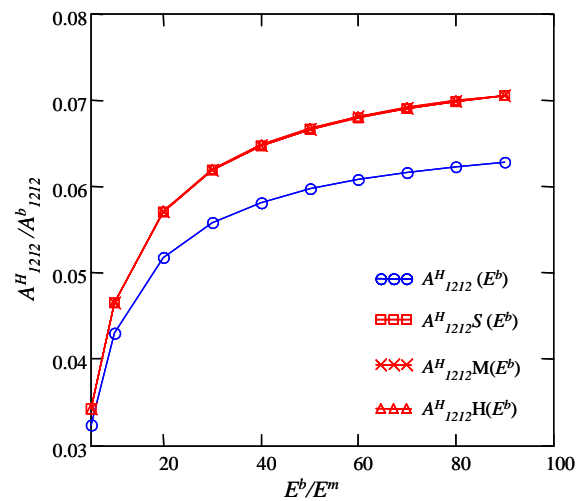


Figure 20 Ratio between A^H_{1212} and A^b_{1212} versus ξ^{-1} comparing un-strengthened and strengthened masonry.

However, the positive contribution of CFRP repointing is evident. The bed joint stiffness is increased along y_1 axis direction and the transversal elongation is reduced so that less tensile stress are transmitted from mortar bed joint to blocks. The FRP axial stiffness has to be taken into account only

to increase the strengthened masonry stiffness along horizontal joint. The in plane stiffness increment is about 20÷60 % in function of masonry parameters (block and mortar stiffness) and FRP mechanical properties. This latter depends on the nature of the fibre used in the CFRP strengthening.

The sensitivity of CFRP repointing technique is evaluated as:

$$\Delta A_{\alpha\beta\gamma\delta}^H = \frac{A_{\alpha\beta\gamma\delta}^H(FRP) - A_{\alpha\beta\gamma\delta}^H}{A_{\alpha\beta\gamma\delta}^H(FRP)} \cdot 100 \quad (17)$$

where $A_{\alpha\beta\gamma\delta}^H(FRP)$ is the in plane moduli for strengthened masonry and $A_{\alpha\beta\gamma\delta}^H$ is the in plane moduli for un-strengthened masonry.

In figure 21, the $A_{\alpha\beta\gamma\delta}^H$ in plane modulus is plotted versus the ξ^{-1} ratio, considering slow (S), medium (M) and high (H) longitudinal Young modulus of FRP for A_{1111}^H , whereas only the slow modulus is considered for the other moduli. The A_{1111}^H in plane stiffness reduces when the ξ^{-1} ratio increases in function of the E_{FRP} parameter, whereas the A_{2222}^H , A_{1122}^H and A_{1212}^H in plane stiffnesses increase slowly in the full range, showing more evident increment for small ξ^{-1} ratio.

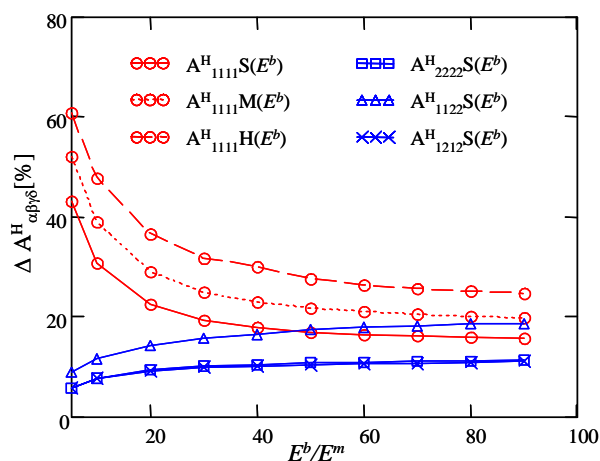


Figure 21 $\Delta A_{\alpha\beta\gamma\delta}^H$ increment of in plane stiffness for strengthened masonry in comparison with un-strengthened one.

8 Masonry panel

A 2D heterogeneous F.E. model has been built to represent infill running bond masonry panel. The aim is to compare the 2D heterogeneous model with the 2D homogenised model. Plane elements (4 node) are used in modelling 2D heterogeneous F.E. model of masonry panel, both for blocks, mortar joints and CFRP repointing (Fig. 22).

The masonry panel is $H=1160$ mm height and $B=1550$ mm width. Bed and head joints thickness is 10 mm, whereas the block are $250 \times 120 \times 55$ mm³ in

the un-strengthened panel, whereas in the strengthened panel bed joint is composed of: one layer of mortar joint (4.4 mm), one layer of FRP (1.2 mm) and one layer of mortar joint (4.4 mm). The total thickness of bed joint is still 10 mm, according to section 5.

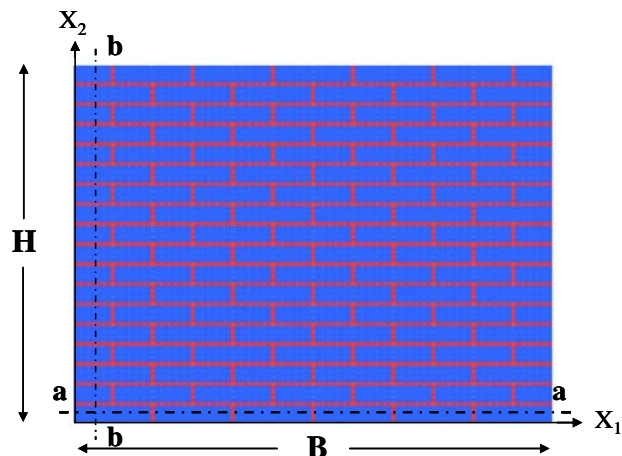


Figure 22 2D heterogeneous numerical model.

The panel is firstly loaded by an unit horizontal displacement at the top ($u_1=1$ mm) along axis x_1 , whereas the base is fixed ($u_1=0$; $u_2=0$); secondly the panel is loaded by an unit vertical displacement at the right side ($u_2=1$ mm) along axis x_2 , whereas the left side is fixed ($u_1=0$; $u_2=0$). The comparison between the 2D heterogeneous F.E. model and 2D homogenised model is carried out for $10 \leq \xi^{-1} \leq 90$. Under plane strain hypothesis, the numerical analysis has been carried on comparing the results of the F.E. heterogeneous masonry panel and with those obtained by the F.E. homogenised model, with the same mesh, which in plane moduli are those evaluated in the section 7.2. The same analysis was conducted for strengthened masonry panel, evaluating the effect of slow, medium and high FRP longitudinal Young modulus.

Considering the first boundary and loading ($u_1=1$ mm) conditions, the ϵ_{22} vertical strain of the cross section at 100 mm and 125 mm from the base is considered (Fig. 22, section a-a). The first cross section considers a layer of blocks (B) and vertical joints; the second cross section considers a layer of mortar joint (J) or mortar joint/FRP (J -FRP) as shown in figure 23.

The numerical results carried out show that a good agreement between 2D heterogeneous model and 2D homogenised model for both un-strengthened and strengthened cases.

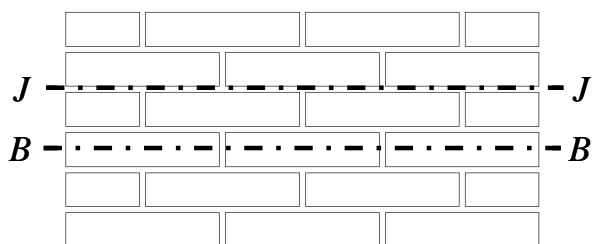


Figure 23 Detail of cross sections in masonry panel.

In figure 24, the results carried out by the two procedures of homogenisation, analytical (AN) and numerical (NUM), are compared with the heterogeneous case for $\xi^{-1}=50$. The diagram shows in ordinate the ε_{22} strain while in abscissa the position in the cross section. As expected, in the heterogeneous model the diagram is characterised by pick points due to the disposition of head joints; hence, to compare the diagram with the ones obtained from homogenised models the effective diagram is interpolated.

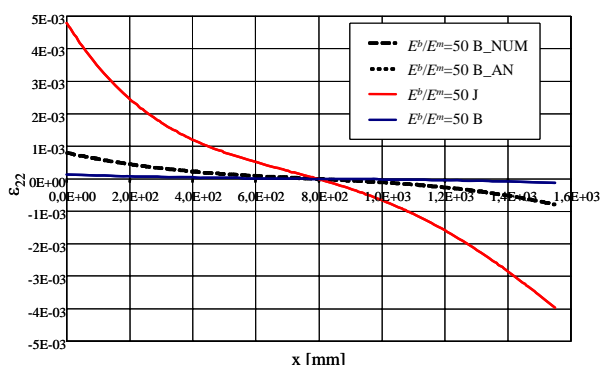


Figure 24 ε_{22} in layers B and J, in 2D heterogeneous model and 2D homogenised model, evaluated by analytical and numerical homogenisation procedure.

The homogenised model is included between the strain distribution at B layer and J layer of the heterogeneous model; the homogenised solution is more close to B layer distribution because the percentual area of block is bigger than that of joint and this is more evident when the ξ^{-1} ratio increases. The 2D homogenised model has the same strain distribution along B layer and J layer due to the assumptions of homogenised masonry model; so that only B layer is considered for this model.

The investigation has been carried on considering the strain distribution along section a-a and b-b (Figure 22), considering respectively the brick layer (Figure 23) and the two boundary conditions reported in table 3 and 4.

$x_1 = 0$	$x_1 = B$	$x_2 = 0$	$x_2 = H$
$u_1 \neq 0$	$u_1 \neq 0$	$u_1 = 0$	$u_1 = 1\text{mm}$
$u_2 \neq 0$	$u_2 \neq 0$	$u_2 = 0$	$u_2 = 0$

Table 3: 1st boundary conditions for F.E. model.

$x_1 = 0$	$x_1 = B$	$x_2 = 0$	$x_2 = H$
$u_1 = 0$	$u_1 \neq 0$	$u_1 \neq 0$	$u_1 \neq 0$
$u_2 = 0$	$u_2 = 1\text{mm}$	$u_2 \neq 0$	$u_2 \neq 0$

Table 4: 2nd boundary conditions for F.E. model.

The ε_{11} , ε_{22} and ε_{12} strain distribution for different E_{FRP} has been evaluated by means of 2D homogenised model and plotted in the following diagrams. In abscissa the position in the panel respect to a-a or b-b sections; in ordinate ε_{11} , ε_{22} and ε_{12} strain. In particular in ordinate at left the ε_{22} values are reported, while at right ε_{11} , and ε_{12} values are reported.

The ε_{11} , ε_{22} and ε_{12} strain distribution along section a-a (Fig. 25, 26, 27), obtained considering the 1st boundary condition, shows that:

1. the ε_{11} strain is influenced by the longitudinal Young modulus of the CFRP repointing material;
2. increasing the CFRP modulus the ε_{11} strain values decrease significantly for low value of ξ^{-1} ;
3. the ε_{11} strain is strongly related to the ξ^{-1} ;
4. the ε_{22} and ε_{12} strains are not related strongly to the ξ^{-1} ;
5. the effect of CFRP modulus increment is less when the ξ^{-1} increases.

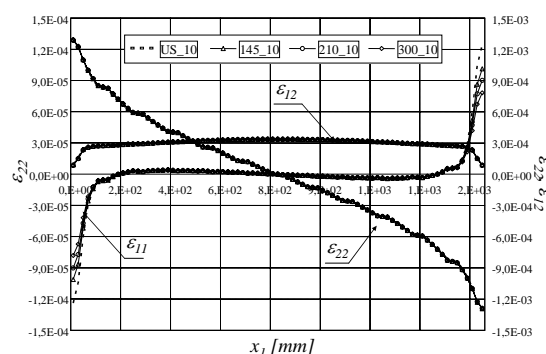


Figure 25 ε_{11} , ε_{22} and ε_{12} strain distribution in section a-a, in 2D homogenised model for $\xi^{-1}=10$.

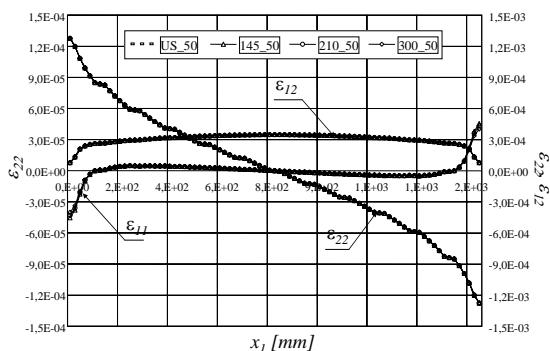


Figure 26 ε_{11} , ε_{22} and ε_{12} strain distribution in section a-a, in 2D homogenised model for $\xi^{-1}=50$.

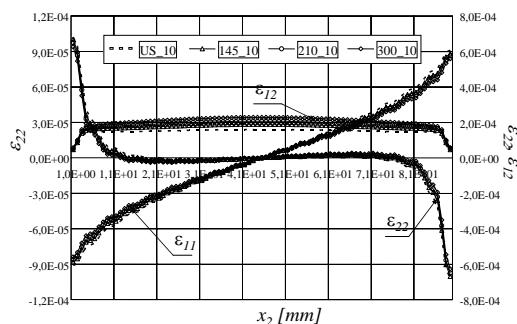


Figure 28 ε_{11} , ε_{22} and ε_{12} strain distribution in section b-b, in 2D homogenised model for $\xi^{-1}=10$.

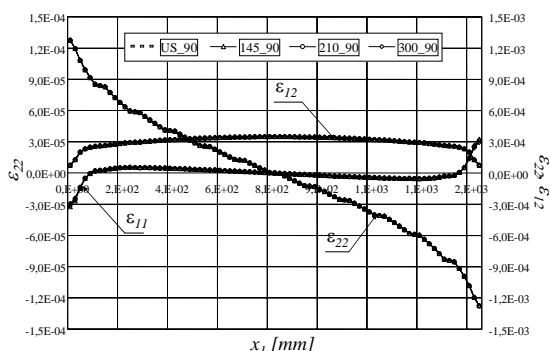


Figure 27 ε_{11} , ε_{22} and ε_{12} strain distribution in section a-a, in 2D homogenised model for $\xi^{-1}=90$.

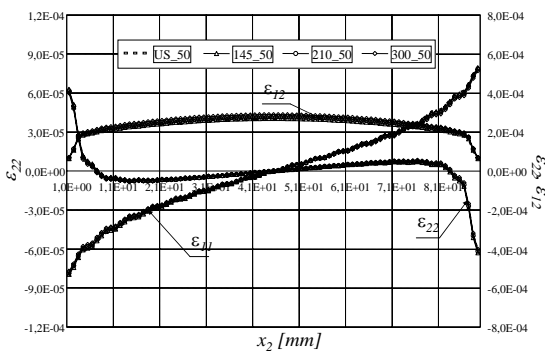


Figure 29 ε_{11} , ε_{22} and ε_{12} strain distribution in section b-b, in 2D homogenised model for $\xi^{-1}=50$.

The ε_{11} , ε_{22} and ε_{12} strain distribution along section b-b (Fig. 28, 29, 30), obtained considering the 2nd boundary condition, shows that:

1. the ε_{11} and ε_{12} strains are influenced by the longitudinal Young modulus of the CFRP repointing material;
2. increasing the CFRP modulus the ε_{11} strain values decrease, whereas the ε_{12} strain increases for low value of ξ^{-1} ;
3. the ε_{22} strain is strongly related to the ξ^{-1} , whereas the ε_{11} and ε_{12} strains are less related to the same parameter;
4. the effect of CFRP modulus increment is less when the ξ^{-1} increases.

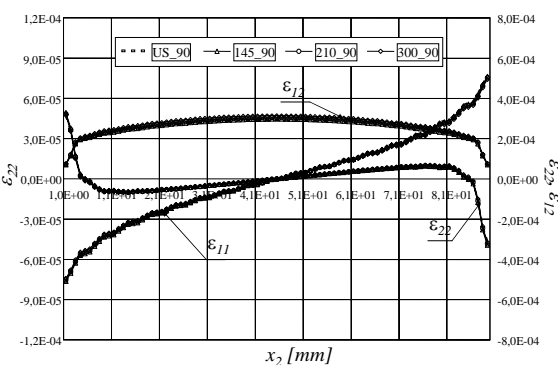


Figure 30 ε_{11} , ε_{22} and ε_{12} strain distribution in section b-b, in 2D homogenised model for $\xi^{-1}=90$.

In figures 31, 32 and 33, the un-strengthened heterogeneous masonry panel is compared with the strengthened one. Three ξ^{-1} ratios has been considered: 10, 50 and 90.

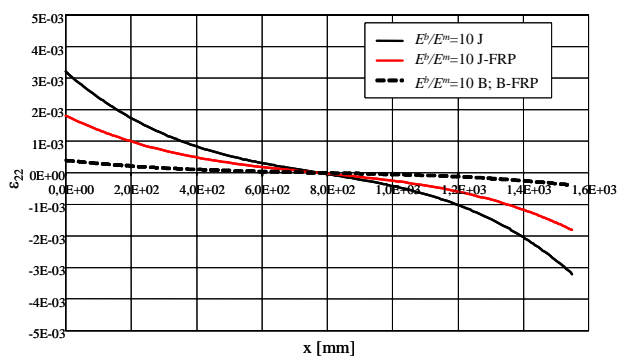


Figure 31 ε_{22} along layers B and J , for $\xi^{-1}=10$ ratio, for 2D heterogeneous model and 2D homogenised FRP model evaluated by numerical homogenisation procedure.

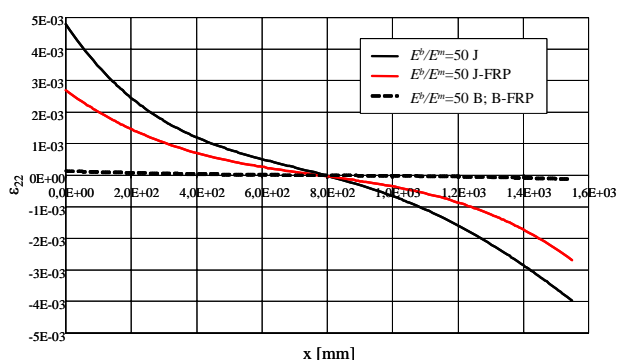


Figure 32 ε_{22} along layers B and J , for $\xi^{-1}=50$ ratio, for 2D heterogeneous model and 2D homogenised FRP model evaluated by numerical homogenisation procedure.

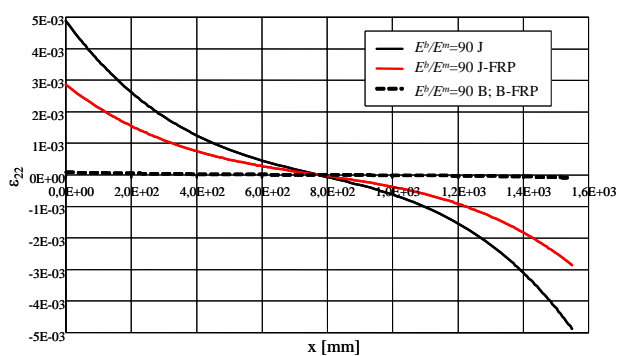


Figure 33 ε_{22} along layers B and J , for $\xi^{-1}=90$ ratio, for 2D heterogeneous model and 2D homogenised FRP model evaluated by numerical homogenisation procedure.

Considering the ε_{22} strain along layers B , as shown in figure 23 no differences exist in un-strengthened and strengthened masonry, whereas along the bed joint the strain distribution is modified by the presence of CFRP repointing. The strengthened bed joint is more stiff so that the strain

values are less than those in the case of un-strengthened bed joint. The stiffness of bed joint is function of ξ^{-1} ratio and it is not influenced by E_{FRP} . The homogenisation procedure proposed in the present paper provides a significative tool to define the constitutive function of an homogenised material equivalent to the heterogeneous one. The numerical model is able to take into account the CFRP repointing technique, whereas the analytical one has to be implemented for this aspect. Generally the data carried out by the proposed procedure are more reliable for low value of ξ^{-1} . The contribution of CFRP repointing is not much relevant in terms of strain distribution due to the analysis is carried out in the linear elastic field. The procedure has to be developed and extended to the limit analysis.

9 Conclusion

The proposed 2D homogenised model allows to investigate easily the in plane behaviour of masonry panel, when a wider set of internal parameters varies (i.e. relative deformability of the joints, blocks and strengthening materials as its distribution along masonry thickness).

The CFRP repointing technique is a suitable strengthening technique to increase the stiffness of masonry panel for in plane loading. The comparison between F.E. heterogeneous and homogenised models has pointed out the following observations:

- 1- The effect of CFRP repointing technique is more evident for low value of ξ^{-1} .
- 2- The A_{1111} in plane modulus achieves the biggest benefit from strengthening materials. In fact the increment of A_{1111} in plane stiffness is about 40÷60% for high value of ξ^{-1} and 20÷30% for low value of ξ^{-1} .
- 3- The axial stiffness of strengthening material is relevant to define the A_{1111} in plane modulus: high CFRP modulus increases more the in plane stiffness of strengthened panel.
- 4- The A_{2222} , A_{1122} , and A_{1212} in plane moduli are not particularly sensitive to strengthening stiffness. The increment of stiffness respect un-strengthened masonry increases slowly when the ξ^{-1} value increases. The increment of A_{2222} and A_{1212} in plane moduli is no bigger than 10%, whereas that of A_{1122} in plane modulus is no bigger than 20%.
- 5- The strain distribution along strengthened bed joint is more influenced by different E_{FRP} .

The analytical homogenised model shows a good agreement respect to the numerical models. The constitutive functions obtained in a symbolic form

are a very important task to analyse masonry with different mechanical characteristics and different sizes of block and mortar joints, hence the research should be developed evaluating the influence of CFRP repointing. In particular for the strengthened finite joint thickness a model for structured interface should be performed.

The next step may be to implement the analysis by a 3D numerical model that may take into account the behaviour along the masonry wall thickness. The 3D model may be useful to analyse the case of partial strengthening of masonry wall thickness. In fact the analysed strengthening solution (full masonry wall thickness strengthening) is a particular case more applicable in the new constructions than in the historical ones. Generally in the historical masonry walls the CFRP repointing technique concerns few centimetres of masonry thickness.

Another aspect of interest in this research topic is the structural behaviour of out of plane masonry wall strengthened by CFRP repointing. A model of this loading condition is still proposed in [16] for un-strengthened masonry and for masonry strengthened by CFRP sheets [17]. This model may be implemented for strengthened one considering the technique proposed in the present paper. The formulation of a 3D model is the first step to analyse not symmetric strengthening distribution along masonry thickness. The case of not symmetric strengthening may occur in the practical experience, hence in plane and out of plane actions are coupled. In fact sometimes, in the historical heritage, one side of the masonry wall is not accessible to strengthening application, due to the presence of valuable fresco.

Nowadays, the scientific research focuses its interest in the application of homogenisation procedure for limit analysis of masonry structures. In particular some authors applied the homogenisation theory to the limit analysis of running bond masonry texture to define the yield domain [18, 19] and implement this in a F.E. code for the analysis at collapse. Some numerical tests were carried out to verify the model by the limit analysis of a two storeys masonry wall [20]. The proposed model was applied to un-strengthened masonry. Finally the model may be extended to limit analysis for evaluating as the yield domain is modified by the strengthening material and as the different parameters influence the yield domain shape.

Acknowledgments

The research project reported in this paper was conducted with the financial support of CNR-MIUR, SP3, law 449/97.

References:

- [1] D. Tinazzi, M. Arduini, C. Modena, A. Nanni, FRP_Structural repointing of masonry assemblages, *Proc. 3rd Int. Conf. on Advanced Composite Materials in Bridges and Structures*, 2000, pp. 585-592.
- [2] G. Tumialan, P.C. Huang, A. Nanni, P. Silva Strengthening of masonry walls by FRP structural repointing, *Proc. of FRPRCS-5*, 2001.
- [3] L. De Lorenzis, Bond between near-surface mounted fiber-reinforced polymer rods and concrete in structural strengthening, *Structural Journal*, Vol.99, No.2, 2002, pp. 123-132.
- [4] K. Bajpai, D. Duthinh, Bending performance of masonry walls strengthened with near-surface mounted FRP bars, *Proc. of 9th North American Masonry Conference*, 2003, pp. 1052-1062.
- [5] L. Binda, G. Mirabella, C. Poggi, Il campanile del duomo di Monza: valutazione delle condizioni statiche, *L'Edilizia*, 7/8, 1995, pp. 44-53.
- [6] C. Modena, Criteria for cautious repair of historical building, *RILEM: Evaluation and strengthening of existing masonry structures*, 1997, pp. 25-42.
- [7] A. Barbieri, A. Cecchi, Analysis of masonry columns by a 3D F.E.M. homogenisation procedure, *WSEAS Transactions on Applied and Theoretical Mechanics*, Vol.2, No.2, 2007, pp. 42-51.
- [8] A. Cecchi, CFRP reinforced masonry walls: analytical and numerical homogenised models, *WSEAS Transactions on Applied and Theoretical Mechanics*, Vol.1, No.1, 2006, pp. 7-15.
- [9] A. Cecchi, G. Milani and A. Tralli, In-plane loaded CFRP reinforced masonry walls: mechanical characteristics by homogenisation procedures, *Composites Science and Technology*, Vol.64, 2004, pp. 2097-2112.
- [10] A. Cecchi, G. Milani and A. Tralli, Validation of analytical multiparameter homogenisation model for out-of-plane loaded masonry walls by means of the finite element method, *Jour. of Engineering Mechanics*, Vol.131(2), 2005, pp. 185-198.
- [11] X. Zhang, S. Singh, D.K. Bull and N. Cooke, Out of plane performance of reinforced masonry walls with openings. *Journal of*

- Structural Engineering*, Vol.127(1), 2001, pp. 51-57.
- [12] A. Cecchi and K. Sab, A multi-parameter homogenisation study for modelling elastic masonry. *European Journal of Mechanics A/Solids*, Vol.21, 2002, pp. 249-268.
- [13] Eurocode 8, Design of Structures for Earthquake Resistance, Part1: general rules, seismic actions and rules for buildings, Brussels, 2004.
- [14] E.N. Vintzileou, V.A. Palieraki, Perimeter infill walls: the use of bed joint reinforcement or RC tie-beams, *Journal of the British Masonry Society, Masonry International*, Vol.20, No.3, 2007, pp. 117-128.
- [15] A. Cecchi, N.L. Rizzi, Heterogeneous material: a mixed homogeneization rigidification technique. *International Journal of Solids Structures*, Vol.38(1), 2001, pp. 29-36.
- [16] A. Cecchi and K. Sab, Out of plane model for heterogeneous periodic materials: the case of masonry. *European Journal of Mechanics A/Solids*, Vol.21, 2002, pp. 715-746.
- [17] A. Cecchi, G. Milani and A. Tralli, Out-of-plane loaded CFRP reinforced masonry walls: mechanical characteristics by homogenisation procedures, *Composites Science and Technology*, Vol.65, 2005, pp. 1480-1500.
- [18] G. Milani, P.B. Lourenço, A. Tralli, Homogenised limit analysis of masonry walls. Part I: Failure surfaces, *Computers Structures*, Vol.84(3-4), 2006, pp. 166-180.
- [19] G. Milani, P.B. Lourenço, A. Tralli, Homogenised approach for the limit analysis of out-of-plane loaded masonry walls. *J. Structural Engineer, ASCE*, Vol.132(10), 2006, pp. 1650-1663.
- [20] G. Milani, A simple equilibrated homogenization model for the limit analysis of masonry structures. *WSEAS Transactions on Applied and Theoretical Mechanics*, Vol.2, No.5, 2007, pp. 119-125.